

Time-resolved cathodoluminescence study of carrier relaxation in strained $(\text{InP})_2/(\text{GaP})_2$ quantum wires

D. H. Rich^{a)} and Y. Tang

Department of Materials Science and Engineering, Photonic Materials and Devices Laboratory,
University of Southern California, Los Angeles, California 90089-0241

(Received 30 July 1996; accepted for publication 7 October 1996)

The carrier relaxation kinetics and nonlinear optical properties of strain-induced laterally ordered $(\text{InP})_2/(\text{GaP})_2$ quantum wire (QWR) samples were examined with time-resolved cathodoluminescence. A temperature dependence of the QWR luminescence decay time reveals that thermal activation of carriers in the QWR and transfer to and from $\text{In}_{0.49}\text{Ga}_{0.51}\text{P}$ barriers plays an important role in determining the measured lifetimes. The presence of disorder in the QWRs was found to induce inhomogeneous regions which exhibit large variations in carrier capture and band filling. © 1996 American Institute of Physics. [S0003-6951(96)02950-6]

The use of strained-layer epitaxy has recently shown great promise for the formation of nanostructures (quantum wires and dots). The implementation of nanostructures in lasers leads to a lowered lasing threshold currents, owing to a spikelike density of states (DOS) that yields a much narrower and higher peak gain as compared to quantum well lasers.^{1–4} Recently, quantum wires (QWRs) have been fabricated by a strain-induced lateral ordering (SILO) process which occurs spontaneously when $(\text{GaP})_n/(\text{InP})_n$ and $(\text{GaAs})_n/(\text{InAs})_n$ short-period superlattices are grown on GaAs(001) and InP(001), respectively.^{5–9} A lateral modulation of the In and Ga compositions, by as much as ~30%, has been observed in transmission electron microscopy (TEM) and energy dispersive x-ray spectroscopy (EDS) studies.^{6,7}

Nonlinear optical properties in such structure are expected to be enhanced due to the narrowing of the DOS in a two-dimensionally confined system. One important nonlinear optical property is the change in the emission of light (in energy, polarization, and intensity) that results from phase-space filling of carriers.⁸ In this letter, we examine the nonlinear optical effects and carrier relaxation kinetics of $(\text{InP})_2/(\text{GaP})_2$ QWR samples using time-resolved CL. In particular, we examine the extent to which defects and deviations from ideal QWR ordering will alter the optical properties.

Bilayer superlattice (BSL) structures were grown by metal-organic chemical vapor deposition (MOCVD) at the Spire Corporation. First, a 3000 Å $\text{In}_{0.49}\text{Ga}_{0.51}\text{P}$ buffer layer was grown on a GaAs(001) substrate misoriented 3° toward (111)A. Each $(\text{InP})_2$ and $(\text{GaP})_2$ bilayer was grown in a time interval of ~10 s, after which the system was purged to prepare for the succeeding layer. A total of 20 periods of $(\text{InP})_2/(\text{GaP})_2$ were grown giving a thickness of ~200 Å. Finally, a 3000 Å $\text{In}_{0.49}\text{Ga}_{0.51}\text{P}$ capping layer was grown. A schematic of the structure and band diagram resulting from the composition modulation is shown in Fig. 1. Two samples (labeled as 2979 and 2980) were grown with nominally the same growth conditions. As evidenced by the data to be presented below, slight variations in the growth conditions oc-

curred, yielding difference in the optical quality between the samples. Cross-sectional TEM revealed that the composition modulation occurred along the [110] direction with a period of ~800 Å, yielding ~400 Å × 200 Å QWRs. The excitation and temperature dependence of the polarization anisotropy of the QWRs (sample 2979) were found to be consistent with a band-filling model that is based on a $\mathbf{k} \cdot \mathbf{p}$ and 2D quantum confinement calculation.⁸

The time-resolved CL experiments were performed with a modified JEOL-840A scanning electron microscope using the method of delayed coincidence in an inverted single photon counting mode, with a time resolution of ~100 ps.¹⁰ Electron beam pulses of 50 ns width and 10 keV beam energy with a 1 MHz repetition rate were used to excite the sample. The luminescence signal was dispersed by a 1/4 m monochromator and detected by a cooled GaAs:Cs photomultiplier tube (PMT). Time-delayed CL spectra were acquired with a spectral resolution of ~1 nm.

Constant excitation and time-resolved CL spectra were acquired as a function of probe current, as shown in Figs. 2 and 3 for samples 2979 and 2980, respectively. In the wavelength range $620 \leq \lambda \leq 750$ nm, two features originating from the QWR and $\text{In}_{0.49}\text{Ga}_{0.51}\text{P}$ bulk (i.e., the buffer and capping layers) are observed in both samples. Monochromatic CL imaging of the QWR emission from these samples were previously performed.⁹ The CL image for sample 2979 shows an optically homogeneous image mostly free of defects and a single narrow peak corresponding to the QWR emission in

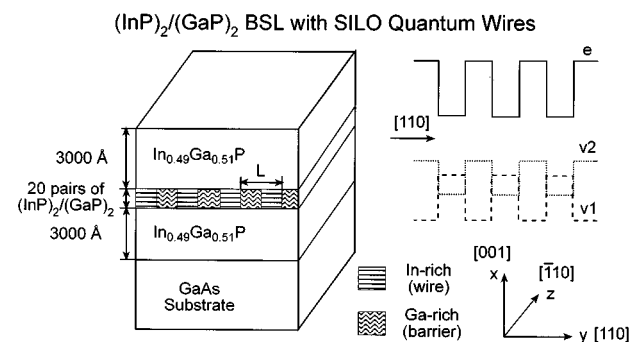


FIG. 1. A schematic diagram of the $(\text{InP})_2/(\text{GaP})_2$ BSL and type-I to type-II superlattice modulation for e-v1 and e-v2 transitions.

^{a)}Electronic mail: danrich@alnitak.usc.edu

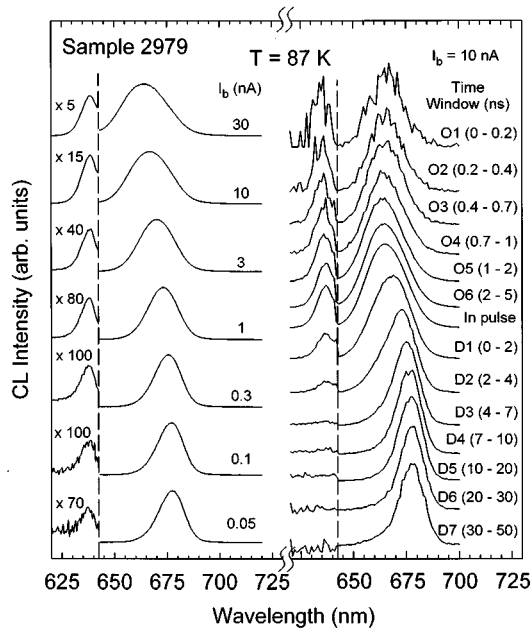


FIG. 2. Stack plots of constant excitation CL spectra for various probe currents (left side) and time-delayed CL spectra in various time windows (right side) for sample 2979.

the CL spectra. On the other hand, the CL image of sample 2980 shows a spotty disorder pattern, exhibiting a high-defect density of 10^7 – 10^8 cm $^{-2}$. The presence of these defects is tied to the quality of the starting surface and initial stages of growth on the GaAs substrates,⁹ and may form as a result of the agglomeration of In on the GaAs surface.¹¹ This sample also shows a broad multicomponent peak in the spectral range corresponding to the QWR emission ($650 \leq \lambda \leq 750$ nm).

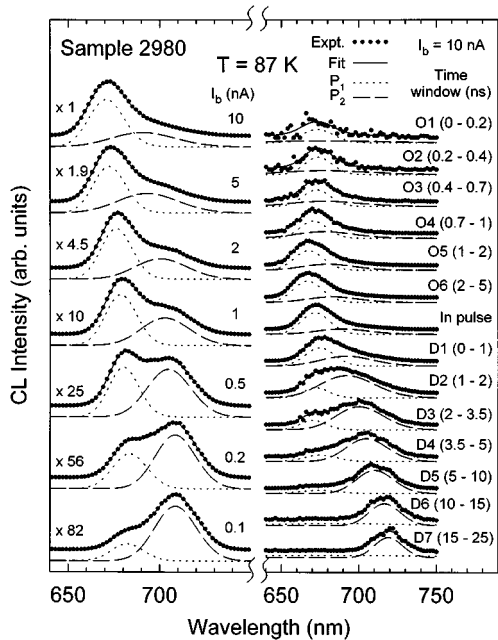


FIG. 3. Stack plots of constant excitation CL spectra for various probe currents (left side) and time-delayed CL spectra in various time windows (right side) for sample 2980. The decomposition of the QWR spectra into two components, P_1 and P_2 , is shown.

The peak energy of the $\text{In}_{0.49}\text{Ga}_{0.51}\text{P}$ bulk emission remains almost constant at ~ 1.950 eV (~ 636 nm) for the different probe currents in both samples (as shown for 2979 in Fig. 2). Emission from the QWR has a lower energy compared to that from the $\text{In}_{0.49}\text{Ga}_{0.51}\text{P}$ layers, as the lateral composition modulation along [110] results in ~ 400 Å \times 200 Å QWRs composed of an In-rich $(\text{GaP})_2/(\text{InP})_2$ BSL region. For sample 2979, the QWR peak energy shifts from 1.834 to 1.869 eV (676 to 663 nm) as I_b increases from 50 pA to 30 nA, as observed in Fig. 2. A significant broadening of the QWR peak (40 to 70 meV) is also observed over this e-beam current range. This nonlinear optical behavior shows that the confined states in the QWR can be filled by a fairly low electron beam excitation. The SILO formation of QWRs in the BSL evidently leads to this enhanced phase-space filling and nonlinear optical effects.

In order to examine the relaxation and collection of carriers into the QWRs, we have measured time-delayed CL spectra at $T=87$ K for the various time-windows indicated in Fig. 2. The time windows O1-O6 and D1-D7 denote time windows relative to the beginning of *onset* and *decay*, respectively, of the luminescence, as referred to the beginning and end of the electron beam pulses. The ratio of the integrated CL intensities of the QWR ($650 \leq \lambda \leq 690$ nm) and $\text{In}_{0.49}\text{Ga}_{0.51}\text{P}$ ($625 \leq \lambda \leq 645$ nm) emissions, $I_{\text{QWR}}/I_{\text{InGaP}}$, increases from 26 to 47 during the onset of luminescence in the O1-O6 time windows. The rapid rise of the QWR peak at the shortest window O1 (centered at 100 ps) reflects the rapid transfer of the carriers into the QWRs, which occupy only $\sim 2\%$ of the material within the e-beam excitation volume. As the time window moves from O1-O6, the QWR peak becomes blue shifted by ~ 3 nm, indicating that carrier filling of the QWR bands and splitting of the quasi-Fermi levels occurs during carrier capture into the QWR. On the other hand, the $\text{In}_{0.49}\text{Ga}_{0.51}\text{P}$ emission shifts to the red by ~ 5 nm in the O1-O6 time windows, reflecting the thermalization and carrier diffusion into lower-energy states of the $\text{In}_{0.49}\text{Ga}_{0.51}\text{P}$ barriers. The spectrum labeled *in pulse*, was taken in the center of the 50 ns wide e-beam pulse, and represents the CL spectrum after carrier generation and recombination has reached steady state, as in the constant-excitation CL spectra of Fig. 2.

During the decay stage of the luminescence, a narrowing and red shifting of both the QWR and $\text{In}_{0.49}\text{Ga}_{0.51}\text{P}$ barrier emissions are observed in the D1-D3 time windows in Fig. 2. As expected, the e-h plasma continuously feeds the lower energy states in both the QWR and barriers as systems proceeds towards equilibrium. The barrier emission decays rapidly in windows D1-D4, owing to the high quantum capture rate into the QWR, as also observed in the onset windows. The CL Intensity vs time transients were taken for various different sample temperatures. An initial luminescence decay time τ is measured from the slopes of the semilogarithmic plots for both the barrier and QWR luminescence and denoted as τ_{InGaP} and τ_{QWR} , respectively. These measurements determined that τ_{QWR} decreases from 2.0 to 1.2 ns, as the temperature increases from 87 to 230 K. The barrier luminescence, on the other hand, has a relatively constant lifetime of $\tau_{\text{InGaP}} = 1.2$ ns over this temperature range. At high temperatures, as in MQW systems,^{12,13} carriers can be thermally

re-emitted from the QWR prior to their recombination. The rate of thermal re-emission of electrons and holes depends on the quasi-Fermi levels and band offsets, which together yield the effective barrier heights. At lower temperatures, fewer carriers are thermally re-emitted, and carriers collected from the barrier recombine mainly in the QWR through radiative recombination. At higher temperatures, additional channels exist for recombination via thermal re-emission from the QWR into the barriers, thereby reducing the measured τ_{QWR} decay time.

As in the case of the excitation dependence of the homogeneous QWR sample (2979), we should observe marked variations in the QWR spectral lineshape of the optically inhomogeneous sample (2980) upon varying the excitation intensity, as observed in Fig. 3. The electron beam was sharply focused to a region corresponding to a typical *bright* region in the CL image of sample 2980.⁹ The lower energy side of the lineshape is observed to dominate for a reduced beam current of 0.1 to ~ 1 nA, after which, the higher energy side of the spectrum has the larger intensity. We have decomposed the QWR lineshapes into the sum of two Gaussian peaks, P_1 and P_2 , to further quantify the behavior of the CL intensity. The results of the fits are shown in Fig. 3 as solid lines running through the data, and short- and long-dashed lines representing peaks P_1 and P_2 , respectively. As a result of band filling, the intensity of the higher-energy peak, P_1 , increases relative to P_2 with the probe current and indicates that the two luminescence features are within a close physical proximity of $\leq 1 \mu\text{m}$ (a carrier diffusion length) of each other.

Time-delayed spectra, for a typical bright region, are also shown in Fig. 3 and the fits to the sum of two Gaussian peaks, P_1 and P_2 are shown. During the onset of luminescence, the carriers initially relax into regions corresponding to the high-energy peak P_1 . A small red shift of 16 meV together with a gradual rise of the low-energy peak P_2 (short-dashed lines) is observed as the system proceeds from windows O1 to O6. In the decay phase, the relative intensity of P_1 and P_2 reverses as carriers thermalize into the lower energy P_2 states. Carrier feeding into the P_2 states is accomplished by thermal re-emission from the higher energy QWR states of P_1 , diffusive transport over surrounding barriers, and carrier capture into the P_2 states. It is remarkable that the initial carrier relaxation occurs into QWR regions exhibiting the high-energy P_1 states for short onset times of ~ 100 ps. This shows the existence of barriers inhibiting initially diffusive transport and rapid collection into the low-energy P_2 regions. The red shift of both P_1 and P_2 states is

evident during the decay phase since the carrier densities and quasi-Fermi level splitting reduce as the system proceeds towards equilibrium.

The presence of two components in the emission strongly suggest the possibility of two different QWR widths and/or compositions that would give rise to different excitonic energies. The disorder inducing the microstructure during the $\text{In}_{0.49}\text{Ga}_{0.51}\text{P}$ growth apparently affects the details of phase separation and spinodal decomposition during the initial phases of the $(\text{InP})_2/(\text{GaP})_2$ BSL growth. The observation of a partially disordered QWR array, giving rise to two or more distinct emissions is, to our knowledge, a new observation in the SILO work.

In conclusion, time-delayed CL spectra for ordered and disordered $(\text{InP})_2/(\text{GaP})_2$ QWR samples have been examined to connect changes in CL linewidth and position with carrier collection and band filling during the *onset* and *decay* of electron beam pulses. Experiments performed at various temperatures show that thermal activation of carriers in the QWR and transfer to and from the $\text{In}_{0.49}\text{Ga}_{0.51}\text{P}$ barriers plays an important role in determining the measured lifetimes. The presence of disorder in the QWRs was found to induce two dissimilar regions which exhibit marked variations in carrier capture and band filling.

This work was supported by ARO and NSF (RIA-ECS). The authors wish to thank P. Colter and S. M. Vernon of the Spire Corporation for use of their samples.

- ¹A. Yariv, Appl. Phys. Lett. **53**, 1033 (1988).
- ²H. Zarem, K. Vahala, and A. Yariv, IEEE J. Quantum Electron. **QE-25**, 705 (1989).
- ³M. Tsuchiya, J. M. Gaines, R. H. Yan, R. J. Simes, P. O. Holtz, L. A. Coldren, and P. M. Petroff, Phys. Rev. Lett. **62**, 466 (1989).
- ⁴E. Kapon, D. M. Hwang, and R. Bhat, Phys. Rev. Lett. **63**, 430 (1989).
- ⁵K. C. Hsieh, J. N. Baillargeon, and K. Y. Cheng, Appl. Phys. Lett. **57**, 2244 (1990).
- ⁶P. J. Pearah, E. M. Stellini, A. C. Chen, A. M. Moy, K. C. Hsieh, and K. Y. Cheng, Appl. Phys. Lett. **62**, 729 (1993).
- ⁷K. C. Hsieh and K. Y. Cheng, Mater. Res. Soc. Symp. Proc. **379**, 145 (1995).
- ⁸Y. Tang, H. T. Lin, D. H. Rich, P. Colter, and S. M. Vernon, Phys. Rev. B **53**, R10 501 (1996).
- ⁹Y. Tang, K. Rammohan, H. T. Lin, D. H. Rich, P. Colter, and S. M. Vernon, Mater. Res. Soc. Symp. Proc. **379**, 165 (1995).
- ¹⁰D. Bimberg, H. Munzel, A. Steckenborn, and J. Christen, Phys. Rev. B **31**, 7788 (1985).
- ¹¹P. R. Hageman, A. van Geelen, W. Gabrielse, G. J. Bauhuis, and L. J. Giling, J. Cryst. Growth **125**, 336 (1992).
- ¹²U. Jahn, J. Menniger, R. Hey, and H. T. Grahn, Appl. Phys. Lett. **64**, 2382 (1994).
- ¹³K. Rammohan, H. T. Lin, D. H. Rich, and A. Larsson, J. Appl. Phys. **78**, 6687 (1995).